Journal
Journal of Energy Storage, 175

ISSN
2352-152X

Authors
Rutqvist, Jonny
Zhang, Yingqi
Alcolea, Andres
et al.

Publication Date
2026-10-01

DOI
10.1016/j.est.2026.123303

Journal of Energy Storage 175 (2026) 123303

Contents lists available at ScienceDirect

Journal of Energy Storage

journal homepage: www.elsevier.com/locate/est

Research Papers

Insights from a coupled thermo-hydro-mechanical analysis of a layered high-temperature thermal energy storage reservoir

Jonny Rutqvist [a,*], Yingqi Zhang [a], Andres Alcolea [b], Raymi Castilla [b], Peter Meier [b], Patrick Dobson [a]

[a] Lawrence Berkeley National Laboratory, CA, Berkeley, USA
[b] Geo-Energie Suisse AG, Zurich, Switzerland

ARTICLE INFO

Keywords:
High-temperature aquifer thermal energy storage
HT-ATES
Coupled thermal-hydraulic-mechanical (THM) modeling
Geostorage Forsthaus
Fiber optic monitoring

ABSTRACT

Coupled thermal-hydraulic-mechanical (THM) modeling is applied to investigate the performance of a seasonal high-temperature aquifer thermal energy storage operation based on data and conditions from current site investigations at the *Geostorage Forsthaus* pilot project in Bern (Switzerland). The model includes subhorizontal sand lenses of various lengths and dips that are embedded in a low permeability clay matrix. Thermal energy storage is simulated by seasonal injection and withdrawal of hot (up to 90 °C) water from a main well, with reservoir pressure regulated by two auxiliary wells at a distance of about 70 m from the main well. The results show how targeted injection into deeper permeable storage formations, along with active deep well pressure control, can effectively minimize geomechanical impact and the potential risk of damaging subsurface storage and sealing formations, or even surface facilities. With such pressure control, the subsurface mechanical responses are dominated by thermal strain and stress, which can be monitored with subsurface fiber optics. The study demonstrates how coupled THM modeling can be applied for the design of a safe and efficient thermal energy storage operation, and how subsurface fiber optic monitoring can be applied for performance confirmation, allowing for more confident operational forecasting.

1. Introduction

High-temperature aquifer thermal energy storage (HT-ATES) refers to the temporary storage of thermal energy in aquifers at high temperatures (i.e., >60 °C) ([1–4]). The main advantage of HT-ATES compared to low-temperature ATES (<30 °C) is that the higher temperature allows the recovered heat to be used directly for heating purposes, and makes the system suitable for more applications, including industrial processes and district heating, without or with less need for additional heat pumps to increase the temperature [2]. Another advantage of HT-ATES is that more energy per cubic meter of water can be stored and retrieved (i.e., higher heat content), enabling lower water mass flow rates to achieve the desired energy supply rate. HT-ATES can be particularly favorable in connection with energy sources that are not controlled by immediate energy demand, such as waste residual heat from power plants and renewable energy sources like geothermal [2,4]. However, injecting hot fluids into the subsurface could induce significant geomechanical changes [5,6]. In HT-ATES, there are concerns that geomechanical changes could lead to potential damage to the storage and sealing formations and subsurface wells, as well as excessive ground surface uplift [7–10]. These geomechanical changes are driven by strongly coupled thermal-hydraulic-mechanical (THM) processes that are best analyzed with numerical modeling.

Coupled THM numerical modeling can be used to predict the performance of an HT-ATES system before implementation and to help understand the key factors influencing the system [7,9–14]. Site characterization data, when available, can constrain the model to reduce prediction uncertainties and refine the design to reduce risks. Monitoring data collected during operation can be used to calibrate the model to further reduce uncertainty in model predictions. Eventually, such a calibrated, site-specific model can be used to evaluate the system performance and help adjust storage operations to optimize performance [10,11,15]. Unlike most conventional geothermal energy reservoirs, these systems rely on localized permeable structures in porous media rather than extensive preferential fracture flow paths [12]. The transmissivity of such localized permeable structures is critical to the

* Corresponding author.
E-mail address: jrutqvist@lbl.gov (J. Rutqvist).

https://doi.org/10.1016/j.est.2026.123303
Received 2 November 2025; Received in revised form 18 May 2026; Accepted 22 June 2026
Available online 27 June 2026

economic viability of an HT-ATES site, particularly when optimizing storage capacity under geomechanical constraints [10,11].

The objective of this study is to apply coupled THM modeling to analyze the performance of an HT-ATES operation in a shallow layered reservoir and to investigate methods for monitoring such an HT-ATES system. The THM analysis includes evaluation of geomechanical responses caused by temperature and pressure changes and strategies to design the system to minimize the potential risk for damaging the system. Potential damage could involve fracturing or shearing that may lead to damaged wells or excessive fluid migration beyond the reservoir and ground uplift. Previous coupled THM modeling and field observations of analogue underground engineering activities, such as geothermal energy operations, typically show that temperature changes dominate local stress and strain near the wells, while fluid pressure can quickly impact larger volumes and can therefore dominate large-scale deformations and ground surface uplift. This has been found associated with geothermal energy operations with water injection [16], carbon storage injection [17], as well as for HT-ATES [7,9,14]. Thermally driven ground surface deformations could also occur but typically require heating near the ground surface, such as for shallow thermal energy storage caverns [18], steam-assisted hydrocarbon production [5] or near-surface ATES [13]. Thus, the depths and spatial extent of induced pressure and temperature changes are important factors that can impact the design and performance of shallow HT-ATES systems.

For a realistic case of a relatively shallow HT-ATES, this study uses data and conditions from current site investigations at the *Geostorage Forsthaus* pilot project in Bern, Switzerland [19,20,12,21]. The plan at *Geostorage Forsthaus Bern* is to store waste heat from a waste incineration plant, a wood-fired power plant, and a combined cycle gas and steam power plant for seasonal usage, up to a storage temperature of 120 °C. The stored heat would then be fed seasonally into the urban district heating network [22].

The targeted thermal energy storage reservoir at *Geostorage Forsthaus Bern* is located within the Lower Freshwater Molasse (USM), which belongs to the Swiss Molasse Basin, a thick Tertiary sedimentary sequence [19,23]. At the project site the USM is overlain by Quaternary unconsolidated deposits (gravels, sands, clays) more than 150 m thick [20]. The USM consists of alternating layers of sand lenses embedded in clay, resulting in permeable horizontal channels and low vertical permeability [19,20,22,23]. A detailed 3D geologic structural framework along with associated rock properties have been developed from the coring, geophysical logging and injection testing along three wells that have been drilled at the site to date [12,21]. The drilling program involved comprehensive coring, logging, and geochemical sampling. Advanced logging techniques, including gamma ray, neutron, and resistivity logs, were employed to determine porosity distribution and water content. Hydraulic testing was conducted at various depth intervals, enabling a local assessment of transmissivity [21]. Additionally, injection testing was conducted, comprised of a three-month long-term circulation test, as well as shorter step-rate tests, accompanied by strain measurements obtained from optic fibers cemented along the wells [21]. Apart from key hydraulic and thermal properties, this data set includes some geomechanical data such as uniaxial compressive strength (UCS) of claystone, silt and fine to very coarse sandstone. The sediments at the site are discontinuous with uncertain lateral extent of individual permeable sand lenses. This uncertainty has led to the development of two different geologic models representing, in terms of system performance, pessimistic and optimistic scenarios, with longer extent of individual sand lenses in the optimistic case.

A conceptual model of the prospective *Geostorage Forsthaus Bern* storage operation is shown in Fig. 1 with a main well and auxiliary wells [22]. The main well will be used to store and recover thermal energy in the form of hot (up to 120 °C) water at flow rates up to 90 m^3/h. The auxiliary wells will be used to regulate the flow at the storage boundary, maintaining the designed aquifer reservoir pressure and connecting the reservoir to the surface system. The auxiliary wells also function to pull

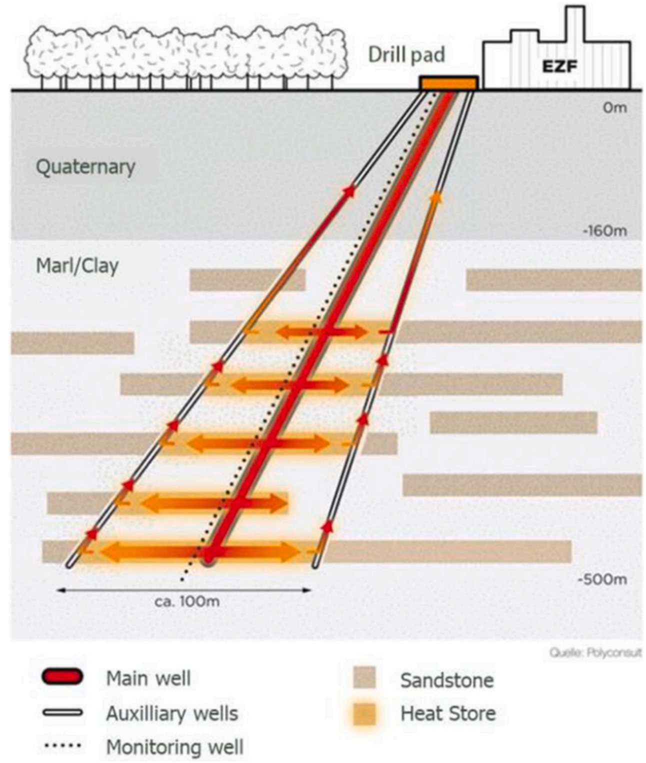

Fig. 1. Conceptual reservoir model for the *Geostorage Forsthaus Bern* pilot project, located beneath the *Energiezentrale Forsthaus* (EZF) power plant, showing sandstone lenses embedded within a matrix composed of marl and claystone [22]. The main well will be used to inject and extract thermal energy in the form of hot water, while the two auxiliary wells will induce fluid circulation and maintain the designed reservoir pressure.

and push the heat plume from and to the main well during heat storage and recovery. The ideal concept is that the underground storage formation, the wells, and the surface facilities will act as a closed circulation system.

A key aspect of this modeling study of the *Geostorage Forsthaus Bern* is to consider the realistic geometry of permeable sand lenses embedded in low permeability clay layers and to understand how these geological units respond mechanically to the thermal and hydraulic loading. Finally, the modeling study aims at investigating how these mechanical responses of the layered storage formation can be utilized to monitor the subsurface performance of the system and how to minimize the potential risk for damaging the subsurface system.

2. Model setup

The THM modeling is conducted with the TOUGH-FLAC simulator for multiphase fluid flow, heat transfer, and geomechanics [24,25]. The simulator is based on the coupling of TOUGH3, a multiphase flow and heat transport simulator [26], and FLAC3D, a geomechanical simulator [27]. TOUGH-FLAC has previously been extensively applied for analysis of coupled THM processes in various high temperature applications, including high-temperature nuclear waste disposal, geothermal energy, and underground thermal energy storage [16,18,28].

The reliability of the TOUGH-FLAC simulator in solving coupled THM processes relevant to HT-ATES has been substantiated through rigorous verification against analytical solutions (e.g., [24,29,30]). Furthermore, the model has been validated against empirical THM laboratory and field data, including in-situ rock heating experiments in argillaceous clay laboratories where temperature, pore pressure, stress, strain, and fracture deformations were closely monitored (e.g., [31–35]). Additionally, previous studies have successfully validated the model against observed ground-surface uplift (e.g., [16,17,36]). These established benchmarks provide high confidence in the model's ability to simulate the thermal and pressure-induced impacts on reservoir deformation, potential fracturing, and surface uplift evaluated for the *Geostorage Forsthaus Bern* site in this study.

In the simulations of the *Geostorage Forsthaus Bern*, the EOS1 fluid equation of state module is applied in TOUGH3 for accurate pressure and temperature-dependent fluid properties [26]. EOS1 handles pure water in liquid, vapor (gas) or two-phase conditions, with fluid properties calculated from the International Formulation Committee (1967) steam table. Important coupled THM processes considered in this TOUGH-FLAC modeling of the *Geostorage Forsthaus Bern* are hot water transport with buoyancy, thermal conduction and advection with the liquid water, heating and thermal expansion of the formations, as well as pressure-induced changes in effective stress.

Fig. 2 shows the three-dimensional model geometry representing the optimistic geological structural model with relatively continuous sand lenses, some of which connect the main well and the two auxiliary wells. As observed, the layering is explicitly included in the THM model with various types of sandstone layers (fine, medium, and very coarse) embedded within a low permeability clay matrix. The main well and one auxiliary well (Aux1) honor the well trajectories of two existing wells at the site, whereas a second auxiliary well (Aux2) was artificially added to ensure sufficient hydraulic connectivity within the most permeable sand lenses, enabling the simulation of an HT-ATES system.

To reduce the overall computational cost, the reservoir model uses a coarser discretization than the geological model, resulting in some diminished and/or partly isolated thin sand layers (consistent with the conceptual sedimentary architecture). The TOUGH-FLAC THM model of dimensions 1246 × 1296 × 280 m consists of about 200,000 elements with cuboid elements of 5 m horizontal side length and vertical thickness of 2 or 5 m in a 200 × 250 × 280 m volume around the wells (Fig. 2). Element sizes gradually increase towards the lateral boundaries to further optimize computational efficiency. Following the same rationale, the Quaternary sediments overlying the USM are not included in the THM model, but included in the FLAC3D mechanical model for calculating ground surface uplift. The sand layers are not exactly horizontal, as observed in the horizontal cross section at −475 m that intersects several inclined sand lenses and the three wells. The wells are explicitly modeled in the TOUGH flow and heat transport simulator, with a well radius of 0.11 m, for the connection area with the formation elements it intersects.

The permeability distribution derived from site investigations is shown in Fig. 2, with sandstone permeability ranging from 5×10^{-15} m^2 to 1×10^{-13} m^2, correlated with porosities ranging from 0.13 to 0.17. However, initial simulations indicated that to sustain the target injection flow rate of 90 m^3/h, the permeability of the main sand layers connecting the wells must be increased by about one order of magnitude, to 3.3×10^{-13} m^2, to avoid excessive reservoir overpressure. At the site, this could potentially be achieved through formation stimulation techniques, though their implementation is beyond the scope of the present THM modeling study. Other important rock properties include thermal conductivity, set to 3.5 W/mK for the saturated sandstone and 2.2 W/mK for clay layers after interpretation of fiber optic temperature profiles, and a standard thermal expansion coefficient of 1×10^{-5} $°C^{-1}$ applied uniformly across all layers.

Mechanical properties such as sediment stiffness and strength were estimated from mechanical test data available after site investigations. A large number of uniaxial compressive strength (UCS) tests were conducted on core plugs taken from cores of the main well and Aux1. Young's modulus (E) was estimated using empirical relations with UCS [37]. For a coarse sandstone with a UCS of approximately 25 MPa, the Young's modulus was estimated to be about E = 5 GPa. For a shale, E = 5 GPa would correspond to a UCS of about 20 MPa. Chang et al. [37] also

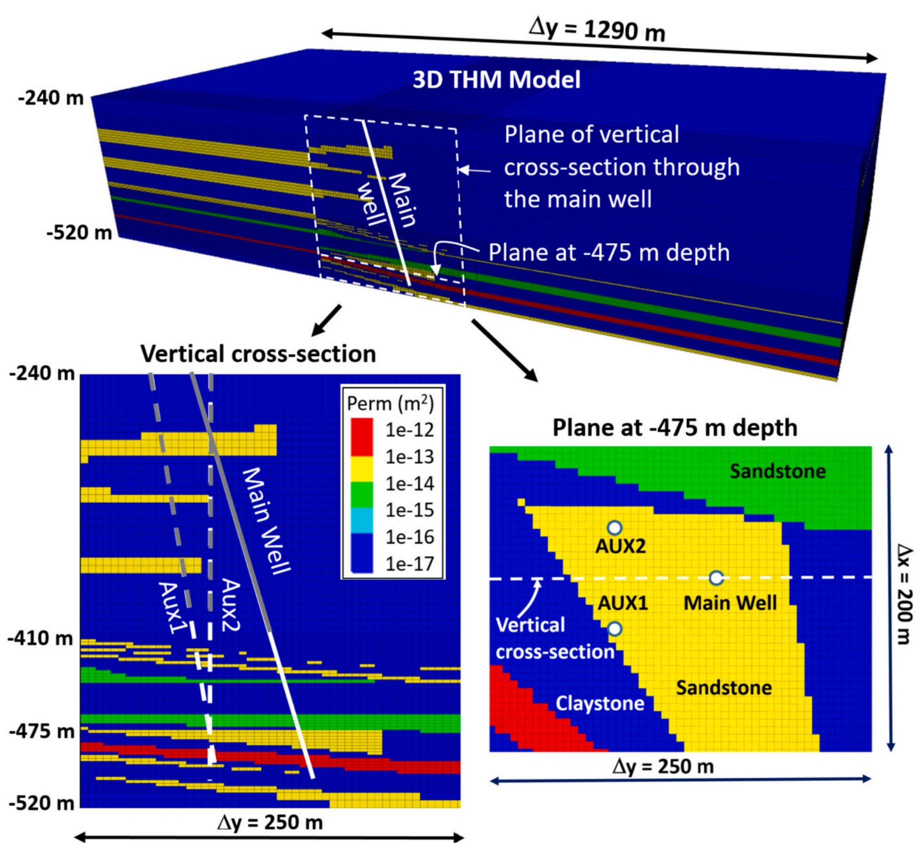

Fig. 2. Cross-sections of the 3D THM model showing the permeability distribution inferred from site investigations: (1) a vertical plane through the main well and (2) horizontal plane at −475 m depth.

developed empirical relations linking strength to porosity and/or gamma ray log responses. Gamma ray values in logs from the *Geostorage Forsthaus Bern* range from about 25 to 75 API, with an average value around 50 API, which, according to Chang et al. [37], correspond to an internal friction angle of 40°. Since there are no indications of major differences in stiffness and strength between the different sediments, E = 5GPa and an estimated Poisson's ratio of 0.3 were applied to all model layers. The measured UCS and estimated internal friction angle are then used to evaluate the potential for compressive (shear) failure of the sediments, while the potential for tensile failure was evaluated by comparing fluid pressure to the least compressive principal stress.

The potential for shear or opening along weaker bedding planes is considered in a mechanical constitutive model that accounts for anisotropic strength along weak horizontal planes. Indeed, step-rate tests with fiber optic strain measurements, described in Meier et al. [21], revealed geomechanical responses in individual horizontal sublayers within the 5 m sandstone unit. These weak bedding units exhibited opening when the injection pressure reached approximately 11.5 MPa, which is close to the lithostatic stress. In the modeling, these weak bedding layers are not explicitly represented but are implicitly accounted for in a continuum constitutive model, specifically a strain-softening/hardening ubiquitous-joint model [27]. This model allows bedding or weak zone opening or shearing to initiate wherever the Coulomb friction or tensile strength criteria are met, which can represent weak sublayers within sandstone units or weak bedding planes within shale units. In these simulations, the weak planes are modeled with zero tensile strength and zero cohesion, and a low friction angle of 20°. For comparison, the Opalinus Clay at the Mont Terri Laboratory (Switzerland) has been characterized with bedding plane properties of 0.5 MPa tensile strength, 2.2 MPa cohesion, and a friction angle of 23° [38]. This suggests that the selected weak plane properties are conservative in terms of the risks of tensile and shear failure along weak planes.

The initial conditions of temperature, fluid pressure, stress, and their depth dependencies were established through an initial vertical equilibrium simulation. A geothermal gradient of 30 °C/km was assumed, with a fixed average temperature of 12.25 °C at the ground surface [19,20]. A hydrostatic pressure gradient was applied, assuming the groundwater table at the ground surface. Initial stresses were assumed isotropic and calculated from the weight of the overburden, considering an average sediment density of 2300 kg/m^3. Under these assumptions, at the depth of the injection (around 500 m), the initial temperature is 27.3 °C, the initial fluid pressure is 4.9 MPa and the initial isotropic stress is 11.3 MPa. The boundary conditions of the lateral and bottom boundaries are no fluid and heat flow along with zero displacement normal to the boundaries. The top boundary at 240 m depth have fixed pressure and temperature, and is free to move mechanically.

A large number of modeling scenarios and sensitivity studies were first carried out to understand the system performance, leading to the selection of a representative case scenario for the study presented in this article. As described above, to achieve the target injection rate of over 20 l/s (72–90 m^3/h), an enhanced permeability, i.e., 3.3×10^{-13} m^2 is assigned to the deeper sandstone lenses (i.e., below −410 m depth). Second, targeted casing perforations are applied to these highly permeable formations. By targeting the perforation and injection on the permeable formations below −410 m, the resulting mechanical changes are confined to depth, thereby minimizing the risk of damaging shallow sealing formations and reducing ground surface uplift. Third, strict pressure control is applied to both injection and withdrawal wells, limiting the reservoir pressure to minimize the potential for formation damage.

The simulations of the *Geostorage Forsthaus Bern* operation are conducted considering yearly (365 days) loading-unloading cycles, with 217 days (about 7 months) of loading and 148 days (about 5 months) of unloading. During loading, water at 90 °C is injected into the main well while equivalent amounts of water are produced from the two auxiliary wells. During unloading, water at 50 °C is injected into the auxiliary wells while hot water is produced from the main well. In our simulations, pressure was controlled at both injection and production wells, and the resulting flow rates were calculated. The injection pressure during loading is set to approximately 2.3 MPa above hydrostatic in the main well while the pressures at the auxiliary wells are maintained at 1.5 MPa below hydrostatic, resulting in a pressure difference of about 3.8 MPa between the main injection well and the auxiliary wells. During unloading the pressures are set 2.3 MPa above hydrostatic in the auxiliary wells while maintained at 1.5 MPa below hydrostatic in the main well. With this injection schedule, the bottom-hole pressure at about 490 m depth peaks at about 7.3 MPa during injection, which is substantially lower than the 11.3 MPa lithostatic stress, thus avoiding the risk of formation fracturing.

3. Simulation results

The TOUGH-FLAC simulation results are presented in the following subsections, focusing on thermal energy storage performance, THM response, and monitoring of the storage operation.

3.1. Thermal energy storage performance

Fig. 3 shows the simulated thermal energy storage performance over a 10-year seasonal operation. In the main well, a flow rate exceeding the targeted 20 kg/s is achieved during the loading periods, while a rate close to 20 kg/s is maintained during unloading (Fig. 3a). Significant thermal breakthrough occurs in the auxiliary wells during loading, with temperatures reaching up to 75 °C, before decreasing to 50 °C during unloading, when injection takes place in the auxiliary wells (Fig. 3b). The heat delivered during each annual unload period exceeds 6 MW$_{th}$ (Fig. 3c).

Fig. 3d shows the roundtrip efficiency corresponding to the heat flow (i.e., thermal power) in Fig. 3c. The roundtrip efficiency is defined as the ratio of energy recovered to the energy injected into the storage system during each annual cycle [39]. Heat fluxes (Eq. 10 of [40]) are model outputs, which are integrated over the loading/unloading periods to determine energy into and out of the storage system over an annual cycle. The roundtrip efficiency is calculated twice, considering the heat flow in/out of the main well only (i.e., the energy recovered through the main well to the energy injected through the main well), and considering all wells. The gradual increase in efficiency over time indicates that progressively less energy is lost to the system, a behavior commonly observed in thermal energy storage analyses. This increase is more pronounced during the first few years and flattens in later years as the system gradually warms and approaches a pseudo-steady state. For the main well only (which represents the primary performance of the heat storage and recovery system), the efficiency levels off at 55%, whereas when considering all wells, over 90% of the injected heat is recovered.

3.2. THM performance

Figs. 4 through 6 present thermal, hydraulic and mechanical responses along the vertical cross section through the main well (Fig. 2). Results are shown at 0.6 years (end of the first loading cycle), 1.0 years (end of the first unloading cycle), 9.6 years (end of the 10th loading cycle) and 10.0 years (end of the 10th unloading cycle).

Fig. 4a shows the temporal fluctuations of temperature within the heated zone and its progressive expansion over the 10-year seasonal storage operation. After 0.6 years, injection of 90 °C water has heated a rock volume extending laterally about 100 m within the most permeable sandstone lenses near the bottom of the main injection well. By the end of the subsequent unloading cycle (i.e. at 1 year), the temperature in these previously heated zones cools to approximately 50 °C, reflecting the injection of cooler water in the auxiliary wells. At 9.6 and 10.0 years, the heated volume has further expanded both vertically and laterally, indicating cumulative heat propagation and storage development with

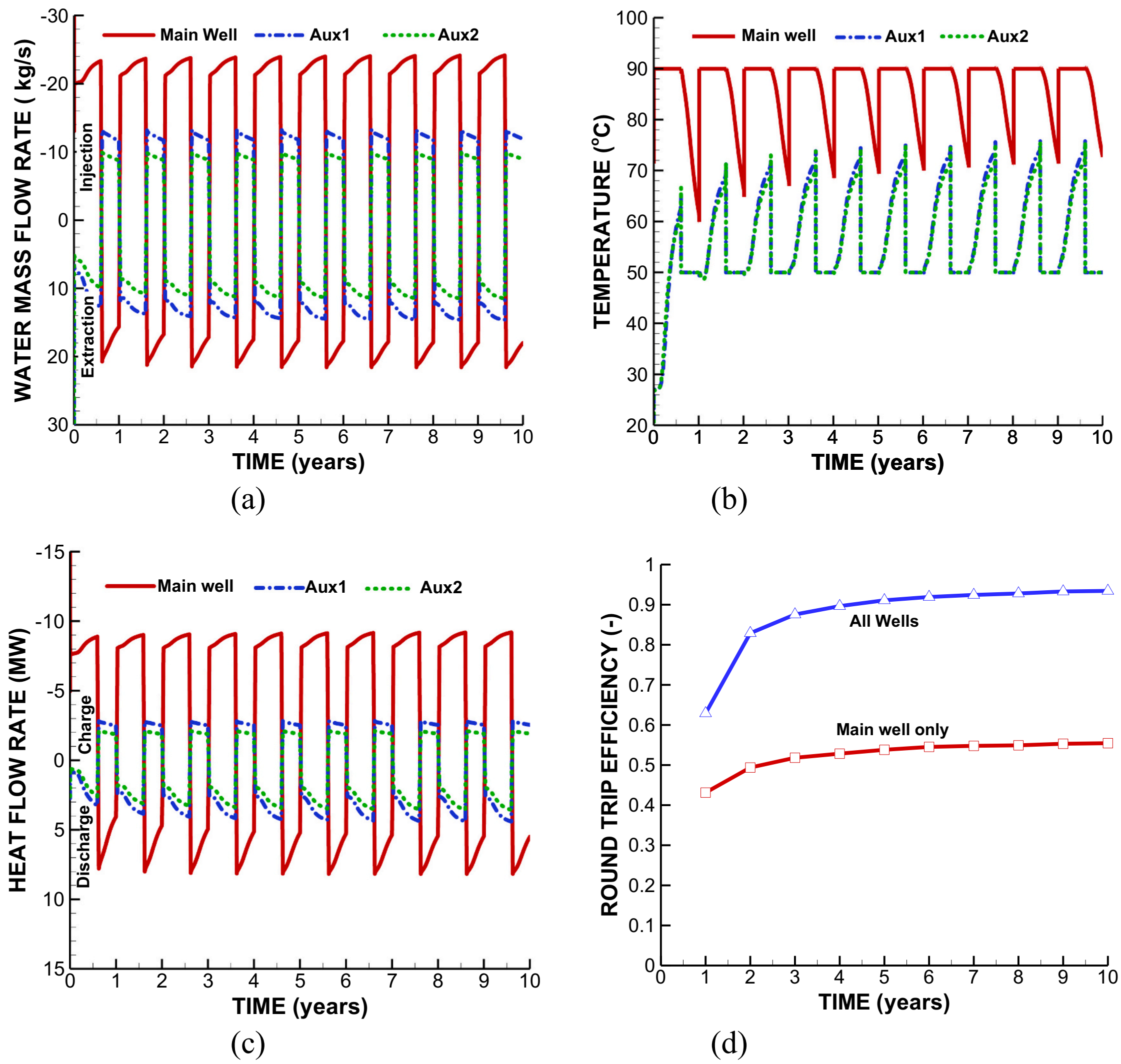

Fig. 3. Simulation results of (a) water mass flow rate, (b) temperature, (c) heat flow rate (i.e., thermal power) and (d) round trip efficiency.

each annual cycle.

Pressure increases at the injection wells and decreases at the extraction wells, resulting in cyclic pressure fluctuations throughout the reservoir (Fig. 4b). Owing to the applied pressure control, these variations remain moderate, less than 2 MPa above or below the initial hydrostatic pressure. The maximum reservoir pressure at depth reaches around 6 MPa, which is substantially below the estimated lithostatic stress of about 11 MPa at reservoir depth, indicating that the operation remains well within safe mechanical limits.

The volumetric strain distribution shown in Fig. 5a exhibits a strong spatial correlation with the temperature distribution in Fig. 4a although some additional strain occurs due to pressure changes adjacent to the wells. The largest volumetric strains occur within high temperature areas, which expand progressively over time. The volumetric strains cause vertical expansion, leading to the vertical displacements illustrated in Fig. 5b. The vertical displacement increases over the 10-year period to a maximum of 30 mm at the top of the heated zone at about −400 m depth. This displacement attenuates upward to less than 10 mm on top of the model at −240 m depth, translating to only a few millimeters of potential ground surface uplift.

Fig. 6 shows the simulated distributions of principal effective stresses. A maximum compressive effective stress of up to 10 MPa develops within the high-temperature zones (Fig. 6a), which remains well below the measured UCS of about 20 MPa. Furthermore, the minimum compressive effective stress remains in compression throughout the simulation and does not approach tensile conditions (Fig. 6b). These results indicate that the considered injection schedule does not induce either shear or tensile failure in the matrix or weak bedding planes. Thus, the analysis indicates elastic mechanical responses and therefore insignificant permanent deformations to the formation.

3.3. Monitoring the system performance

The modeling results show a strong impact of temperature and thermal expansion on subsurface mechanical deformations, particularly on volumetric strain. The simulations also indicate that a small amount of ground surface uplift will occur. However, in a heterogeneous system with complex layering and variable permeability, it can be challenging to attribute such surface uplift to specific subsurface strain zones. In this context, subsurface strain measurements may provide a more effective means of directly monitoring mechanical responses within the layered formation.

For an HT-ATES with injection temperature of 90 °C and pressure fluctuations of a few MPa, the model simulations show that subsurface strain is dominated by thermally-induced strain and stress changes. The dominance of thermally induced strain is evident in Figs. 4a and 5a, which show a strong spatial correlation between temperature and volumetric strain along the vertical plane through the main well. A similar close correlation is also observed on the horizontal plane at −475 m (recall Fig. 2), corresponding to the main heat storage zone

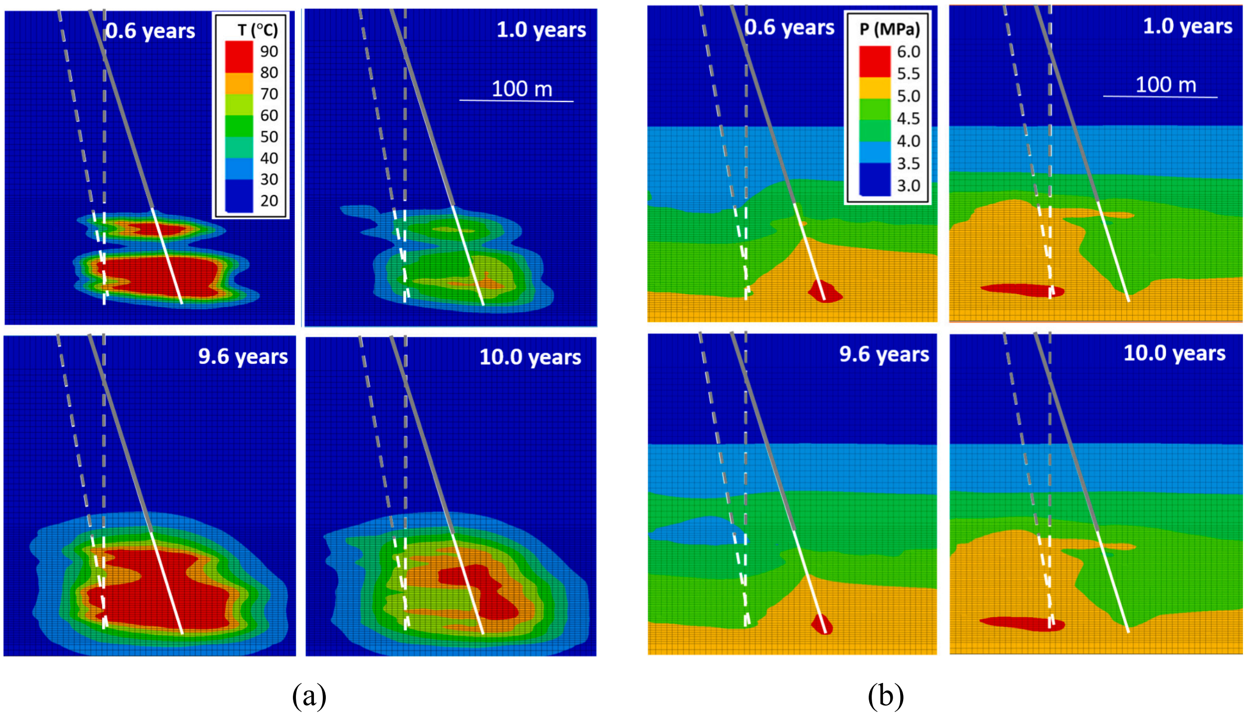

Fig. 4. Vertical cross-section showing simulated (a) temperature and (b) pressure distributions at the end of the 1st and 10th load and unload cycles.

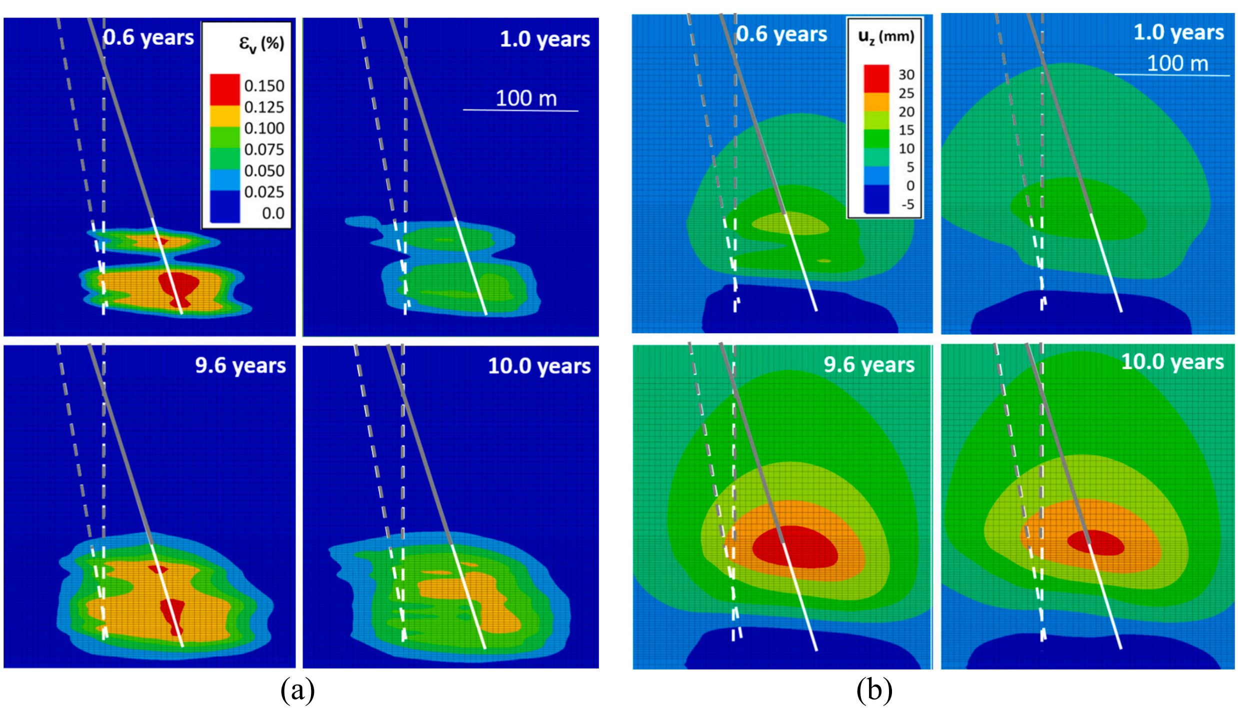

Fig. 5. Vertical cross-section showing simulated (a) volumetric strain and (b) vertical displacement at the end of the 1st and 10th load and unload cycles.

(Fig. 7).

Fig. 8 shows the temperature and the dominant vertical strain along a line parallel to the main well, representing the formation itself. The results reveal again a very close correlation between temperature and strain. For example, in areas reaching 90 °C, the calculated vertical strain is +0.5–0.6 × 10^{-3}. Considering that this corresponds to a 60 °C temperature increase during the first load cycle and applying a thermal expansion coefficient of 1 × 10^{-5} °C^{-1}, the vertical thermal strain can simply be estimated as $\varepsilon_z = 60 \times 1 \times 10^{-5} = 0.6 \times 10^{-3}$, which is consistent with the numerical results in Fig. 8. Just above the heated zone (above −400 m) a slight negative strain (i.e., compression) occurs, caused by compaction in response to the adjacent thermal expansion. Similarly, negative strain is observed in a clay layer at −440 m at 0.6 years. However, this compression is no longer present at 10 years due to the more homogeneous temperature distribution over time.

The observed close correlation between local temperatures, i.e. in

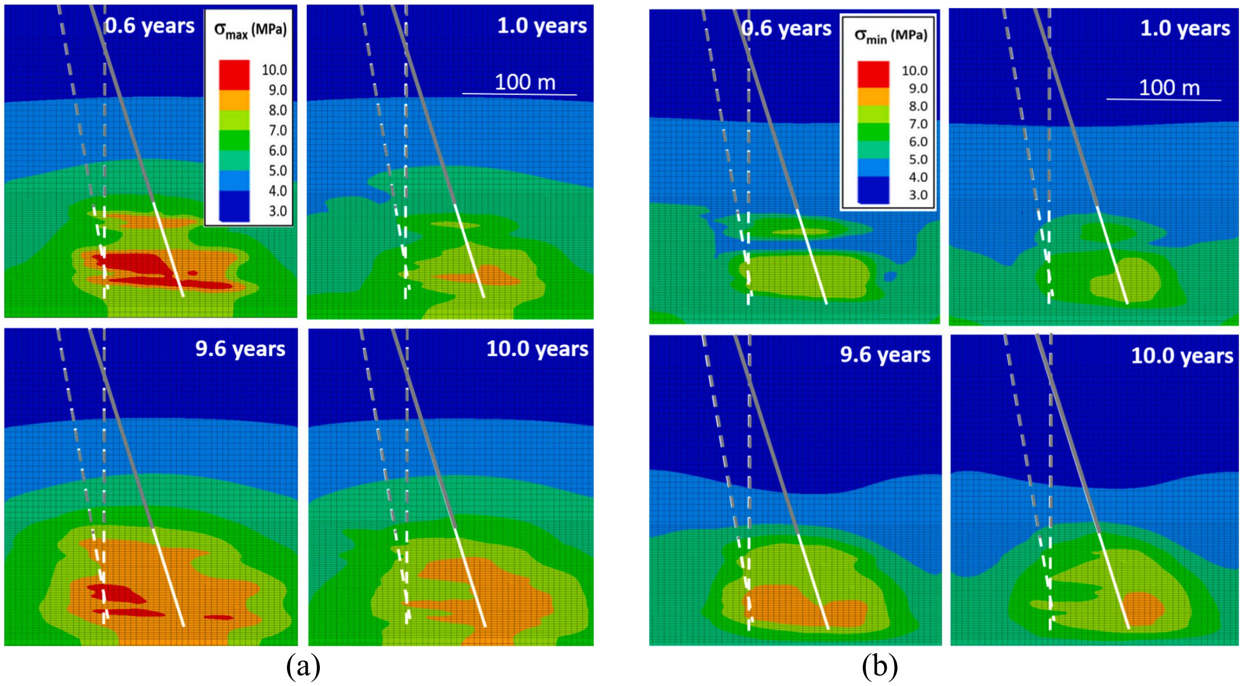

Fig. 6. Vertical cross-section showing simulated (a) maximum compressive principal effective stress and (b) minimum compressive effective stress at the end of the 1st and 10th load and unload cycles.

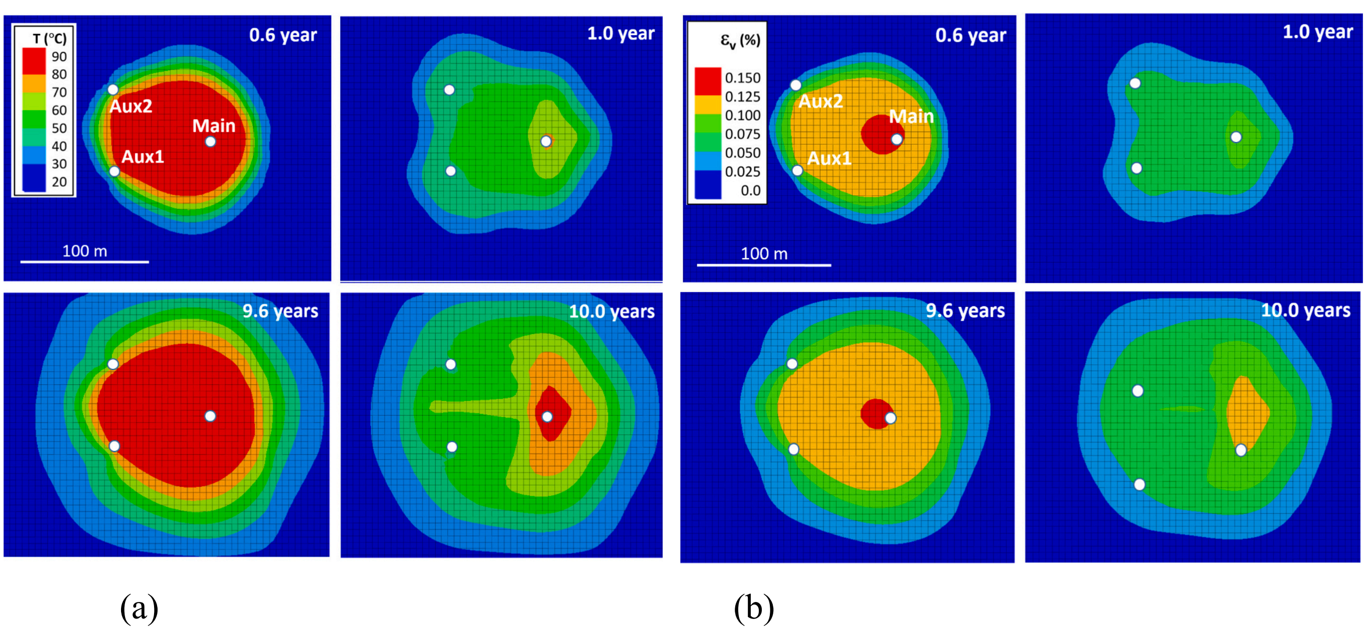

Fig. 7. Horizontal plane at −475 m depth showing simulated (a) temperature and (b) volumetric strain.

regions where heat is stored, and vertical (or volumetric) strain highlights the benefit of using subsurface fiber optic continuous measurements of temperature and strain to monitor the system. Since these measurements should reflect temperature and strain in the formation, rather than those inside the wells, running fiber optics in the well casing cement of the main well, or along a dedicated slim-hole monitoring well may be considered, such as the one illustrated next to the main well in Fig. 1.

To investigate a failure scenario induced along weak bedding planes, a simulation was conducted under very high injection pressure. The results are presented in Figs. 9–11. In this case, the injection pressure was intentionally set so high that the formation pressure exceeded the initial vertical stress (approximately 11 MPa in the reservoir). The simulation results show that parting (opening) of the weak bedding planes occur within the first day of injection near the top of the storage zone (Figs. 9b and 11a). With continued injection, opening of the weak bedding planes also develops in the lower sections of the storage zone, with clearly identified localized strain increments observed by day 30 day (Fig. 10c). While areas reaching 90 °C exhibit a background vertical strain of 0.5–0.6 × 10^{-3}, the localized bedding strains show no correlation with the temperature profile. This decoupling suggests that the localized bedding openings are primarily driven by high pressure exceeding the lithostatic stress (Figs. 9c and 10c). During production, if injection were to continue with the same high pressure in the auxiliary

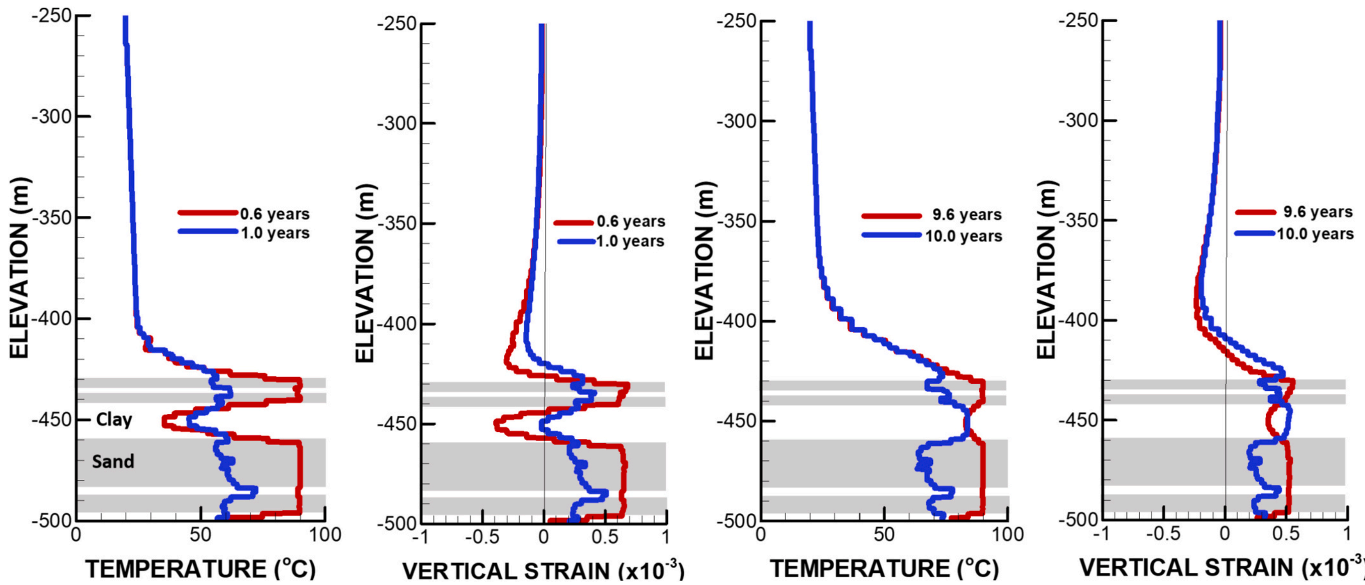

Fig. 8. Temperature and vertical strain of the formation along the main well at 0.6, 1.0, 9.6 and 10 years.

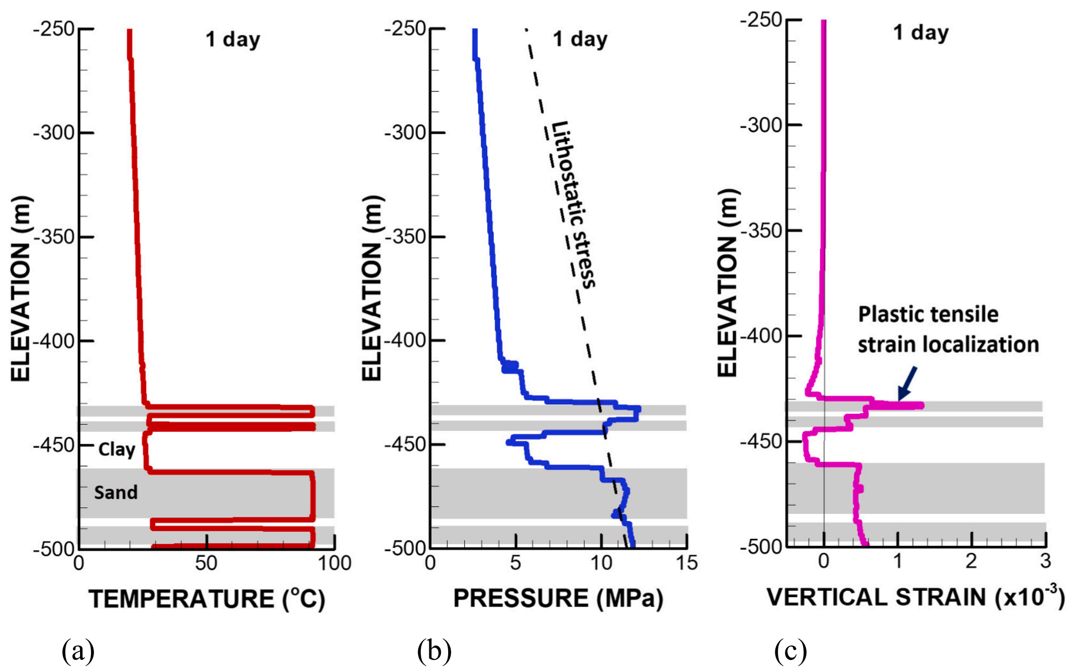

Fig. 9. Results after 1 day of very high pressure injection with profiles of (a) temperature, (b) pore pressure, and (c) vertical strain in the formation along the main well.

wells, extensive opening of weak bedding planes would likely occur, particularly in the uppermost sections of the storage zone (Fig. 11c). Such plastic tensile strain would lead to significant permanent deformations to the formation. Nevertheless, the use of continuous fiber-optic strain and temperature monitoring would allow for the detection of such localized openings within a day of injection, enabling timely preventative actions, such as reducing injection pressure.

4. Discussion

This numerical modeling study was conducted using data and conditions from the current site investigation at the *Geostorage Forsthaus* pilot project in Bern, Switzerland. Following an initial screening and sensitivity analyses, an optimal scenario was simulated that incorporates sand layers with extended lateral extent and sufficient permeability to connect a main heat storage well with two auxiliary wells. Such enhanced permeability could potentially be achieved through traditional reservoir stimulation techniques. The modeled scenario honors the complex layering inferred from site investigations and provides insights relevant to shallow, high-temperature heat storage in layered sedimentary formations.

In terms of efficiency, a 55% roundtrip efficiency for the main well alone may appear low, but this is within the range reported in the literature for other HT-ATES sites [2,41], and in generic mathematical models [1]. Several design modifications could be considered to improve efficiency, such as adjusting injection temperature and/or injection flow rate, adding one or more auxillary wells, or modifying the spacing of the auxiliary wells. The fact that the coupled THM analysis for

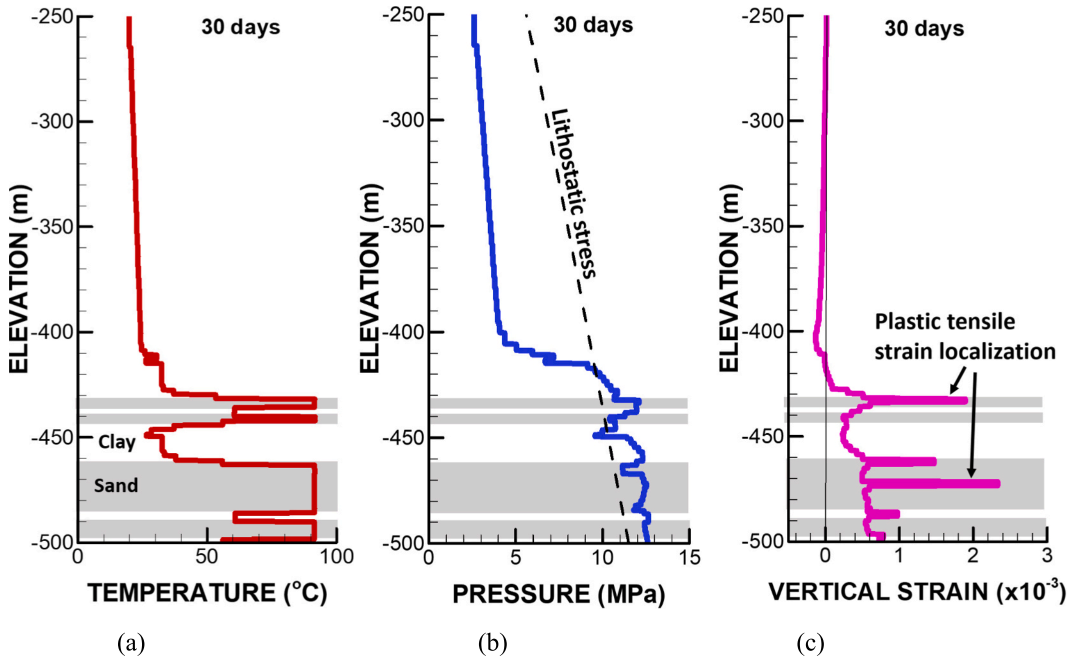

Fig. 10. Results after 30 days of very high pressure injection with profiles of (a) temperature, (b) pore pressure, and (c) vertical strain in the formation along the main well.

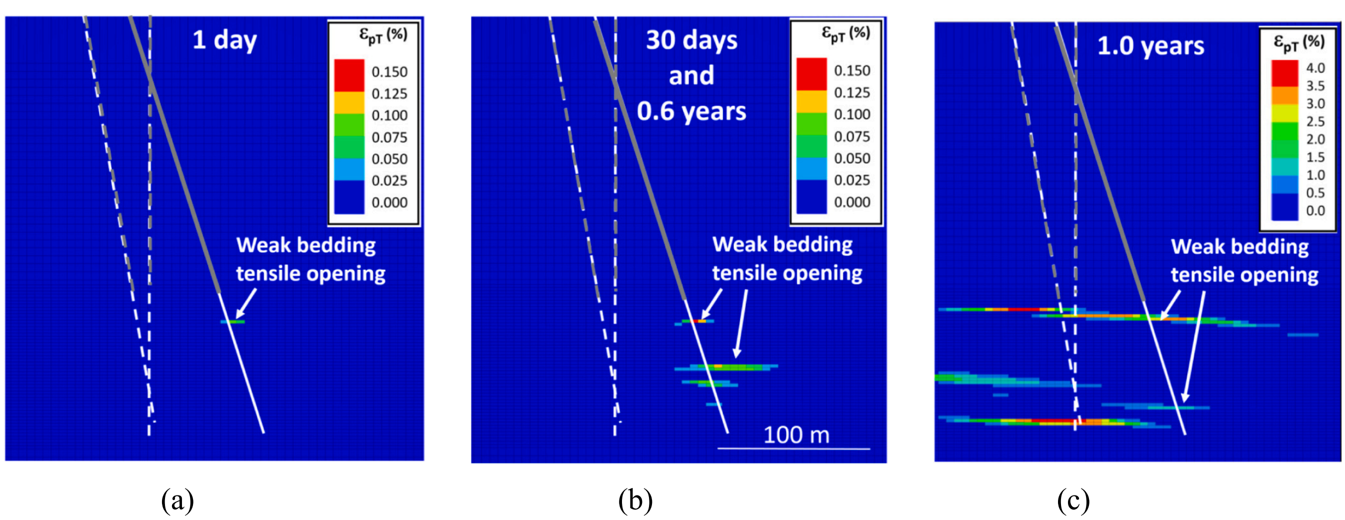

Fig. 11. Results of very high pressure injection showing location of weak plane plastic tensile strain and signifying weak bedding tensile opening after (a) 1 day, (b) 30 days and 0.6 years, and (c) 1.0 years. Note that the weak planes remained constant from 30 days to 0.6 years and are therefore identical as shown in (b).

this case shows that the induced stresses remain far below levels that could cause mechanical damage implies that it would be possible to safely inject at higher temperature and/or flow rates if desired.

The modeling demonstrates that confining targeted perforation and injection to the deeper permeable reservoir sections, combined with strict pressure control, effectively minimizes the risk of mechanical formation damage and limits ground surface uplift. Our base-case simulation with pressure control indicates a maximum vertical expansion of 30 mm at the top of the heated storage zone at −400 m, which is significantly attenuated to less than 10 mm at −240 (Fig. 5b) and results in approximately 4 mm ground surface uplift. A 4 mm ground surface uplift would be unlikely to cause damage to surface infrastructure. By comparison, some previous modeling studies have predicted uplifts exceeding 5 cm [9,14,23]. In those cases, which did not consider strict pressure control as in our study, surface uplift was primarily attributed to reservoir pressure changes. With pressure control, induced thermally induced strains and stresses dominate subsurface mechanical responses, even providing additional confinement and stability to the formation. Over time, as heat diffuses through the low-permeability clay layers, stresses become spatially more homogenous, reducing shear stress and increasing a uniform confining stress. This enhanced confinement lowers the potential for shear along layer interfaces and reduces the risk of pressure-induced fracturing.

Overall, this study demonstrates the value of coupled THM modeling for designing and optimizing energy storage operations, while minimizing the risk of undesired mechanical changes. The results indicate that downhole fiber optic temperature and strain monitoring can be an effective tool for evaluating system performance. Calibrating the model against early-time monitoring data can further support long-term forecasting and allow assessment or optimization of different operational scenarios, such as higher injection rates and/or temperatures. Such comparison with site-specific monitoring data will also provide the ultimate model validation to further reduce model uncertainties. Under normal operation, subsurface strain is expected to closely correlate with temperature, so deviations from this expected behavior could indicate unwanted mechanical changes, including potential hydraulic fracturing or opening of weak bedding planes. In such a case, further detailed investigations may be conducted and preventative measures applied to the injection schedule. Additional monitoring options include fiber optics with distributed acoustic sensing (DAS) for detecting acoustic emissions, providing early warning of potential damage to the formation. These measures can be complemented with surface deformation monitoring to confirm that no fluid migration occurs through the storage overburden.

This study is limited to the geomechanical performance of the reservoir, while features such as wellbore integrity, potential sand production, and geochemical issues are not included. Analysis of wellbore integrity would require a separate model with detailed discretization of the well assembly and its completion, accounting for interfaces and interactions with the formation sediments (e.g. [28]). Considering stress concentrations around a well, some mechanical inelastic yielding could be expected at the borehole walls in contact with the perforated casing, which in turn might result in minor sand production. Geochemical modeling of the Geostorage Forsthaus Bern site, including precipitation or dissolution of calcite and dolomite, is reported in Diaz-Maurin and Saaltink [22] and Vidal and Saaltink [42] and is beyond the scope of the present study. The modeling performed in this study was further limited to homogeneous properties within each sand layer and the clay matrix, using average properties. However, the analysis accounts for significant anisotropy in mechanical strength properties by incorporating horizontal weak beddings with zero tensile strength and low shear strength. Furthermore, a pronounced anisotropy is also captured in the thermal and hydraulic results by representing the subhorizontal layering with high permeability in the sandstone layers. To achieve a feasible scenario with a sufficient circulation rate for storage operations, the permeability was increased. As supported by Meier et al. [21], who reported similar findings based on observations at offset wells in the USM, such high permeability values are not unrealistic and are, in fact, anticipated in this context.

5. Conclusions

The objective of this study was to apply coupled THM modeling to analyze the performance of a high-temperature aquifer thermal energy storage (HT-ATES) system in a shallow, layered reservoir and to investigate methods for monitoring such a system. For a realistic case, the study is based on data and conditions from current site investigations at the *Geostorage Forsthaus* pilot project, in Bern (Switzerland). The main findings, relevant to the coupled THM performance and monitoring of HT-ATES in layered formations, are:

- Targeted casing perforation and injection into deeper storage sediments confines mechanical changes at depth, thereby limiting impacts on shallow seals and reducing ground surface deformation.
- Reservoir pressure control through extraction wells is an effective method to maintain low reservoir pressure changes, thus minimizing the risk of damage to the storage formation and also limiting ground uplift.
- With strict pressure control, subsurface mechanical responses are dominated by thermal expansion, resulting in a strong correlation between local temperature and strain that can be utilized for accurate monitoring of the subsurface storage system.
- Fiber optic temperature and strain monitoring is a viable option to tracking system responses and detect deviations from normal thermal-elastic behavior, which could indicate imminent damage to the storage formation.

Overall, this study demonstrates the value of coupled THM modeling for designing and optimizing HT-ATES operations and performance while minimizing the risk of unwanted mechanical changes. The current model, based on the *Geostorage Forsthaus* pilot project in Bern, shows stress changes well below levels that could cause formation damage, indicating that scenarios with higher injection flow rates and temperatures could be safely explored, provided that strict pressure control and real-time fiber optic monitoring are maintained.

CRediT authorship contribution statement

Jonny Rutqvist: Writing – original draft, Visualization, Software, Methodology, Investigation, Formal analysis, Conceptualization. **Yingqi Zhang:** Writing – review & editing, Software, Methodology, Investigation, Funding acquisition, Formal analysis, Conceptualization. **Andres Alcolea:** Writing – review & editing, Supervision, Investigation, Data curation, Conceptualization. **Raymi Castilla:** Writing – review & editing, Supervision, Resources, Project administration, Funding acquisition, Data curation, Conceptualization. **Peter Meier:** Writing – review & editing, Supervision, Resources, Project administration, Investigation, Data curation, Conceptualization. **Patrick Dobson:** Writing – review & editing, Supervision, Methodology, Investigation, Funding acquisition, Data curation, Conceptualization.

Declaration of competing interest

The authors declare that they have no known competing financial interests or personal relationships that could have appeared to influence the work reported in this paper.

Acknowledgments

We thank the four anonymous reviewers for their helpful comments that improved this paper. This work was supported by the U.S. Department of Energy (DOE), Office of Energy Efficiency and Renewable Energy (EERE), Geothermal Technologies Office, under Contract Number DE-AC02-05CH11231 with Lawrence Berkeley National Laboratory (LBNL), and Contract Number SI/502362-01 of Swiss Federal Office of Energy with Geo-Energie Suisse AG.

Data availability

Data will be made available on request.

References

[1] S. Beernink, N. Hartog, P.J. Vardon, M. Bloemendal, Heat losses in ATES systems: the impact of processes, storage geometry and temperature, Geothermics 117 (2024) 102889.

[2] B. Drijver, M.V. Aarssen, B. de Zwart, High-temperature aquifer thermal energy storage (HT-ATES): sustainable and multi-usable, in: Innostock 2012. 12th International Conference on Energy Storage, 2012.

[3] P. Fleuchaus, B. Godschalk, I. Stober, P. Blum, Worldwide application of aquifer thermal energy storage–a review, Renew. Sust. Energ. Rev. 94 (2018) 861–876, https://doi.org/10.1016/j.rser.2018.06.057.

[4] S. Heldt, C. Beyer, S. Bauer, Uncertainty assessment of thermal recovery and subsurface temperature changes induced by high-temperature aquifer thermal energy storage (HT-ATES): a case study, Geothermics 122 (2024) 103086.

[5] L. Blanco-Martín, J. Rutqvist, C.A. Doughty, Y. Zhang, S.A. Finsterle, C. M. Oldenburg, Coupled geomechanics and flow modeling of thermally induced compaction in heavy oil diatomite reservoirs under cyclic steaming, J. Pet. Sci. Eng. 147 (2016) 474–484, https://doi.org/10.1016/j.petrol.2016.09.002.

[6] P.M. Collins, Geomechanical effects on the SAGD process, in: Society of Petroleum Engineers, SPE Reservoir Evaluation and Engineeering. SPE paper 97905, 2007.

[7] K. Stricker, R. Egert, E. Schill, T. Kohl, Risk of surface movements and reservoir deformation for high-temperature aquifer thermal energy storage (HT-ATES), Geotherm. Energy 12 (2024) 4.

[8] U. Mutlu, A. Ghassemi, D. Adams, G. Boitnott, Geologic thermal energy storage: integrated subsurface characterization and modeling to decode wellbore operability limits, in: 49th Workshop on Geothermal Reservoir Engineering, Stanford University, Stanford, California, 2024.

[9] R. Vidal, S. Olivella, M.W. Saaltink, F. Diaz-Maurin, Heat storage efficiency, ground surface uplift and thermo-hydro-mechanical phenomena for high-temperature

aquifer thermal energy storage, Geotherm. Energy 10 (2022) 23, https://doi.org/10.1186/s40517-022-00233-3.
[10] L. Zhang, Z. Mi, W. Cao, L. Liu, L. Tas, T. Hermans, Multi-objective optimization of energy efficiency and geomechanical safety in high-temperature aquifer thermal energy storage (HT-ATES) systems based on coupled thermo-hydro-mechanical (THM) analysis, Energy 332 (2025) 137096.
[11] D.T. Birdsell, B.M. Adams, M.O. Saar, Minimum transmissivity and optimal well spacing and flow rate for high-temperature aquifer thermal energy storage, Appl. Energy 289 (2021) 116658.
[12] J. Bremer, F. Nitschke, F. Bauer, E. Schill, T. Kohl, E. Kaymacki, T. Koelbel, A. El-Alfy, D. Ollinger, P. Meier, L. Pei, G. Blöcher, S. Klein, F. Hahn, T.A. Atkinson, T. McLing, W. Jin, Y. Zhang, P. Dobson, J. Rutqvist, T. Hörbrand, T. Jahrfeld, VESTA - Very-High-Temperature Heat Aquifer Storage. Proceedings of European Geothermal Congress 2022, Berlin, Germany, 2022.
[13] E.L. Sonnenthal, J.T. Smith, P.F. Dobson, P.S. Nico, Thermal-hydrological-mechanical models for evaluating reservoir thermal energy storage in the Portland Basin, Oregon, in: Proceedings, 46th Workshop on Geothermal Reservoir Engineering, Stanford University, 2021.
[14] Y. Zhang, J. Rutqvist, P. Dobson, E. Schill, A. Alcolea, R. Castilla, P. Meier, T. McLing, W. Jin, T. Atkinson, H. Neupane, A Flow and Geomechanical Study on a High-Temperature Energy Storage Project (VESTA), Geothermal Rising Conference Poster Presentation, Annual Meeting & Expo, Waikoloa, Hawaii, October 27–30, 2024, 2024.
[15] E. Witter, P. Dobson, D. Akindipe, J. McTigue, T. Atkinson, R. Kumar, E. Sonnenthal, G. Zhu, A review of geological thermal energy storage for seasonal, grid-scale dispatching, Renew. Sust. Energ. Rev. 218 (2025) 115761.
[16] J. Rutqvist, P. Jeanne, P.F. Dobson, J. Garcia, C. Hartline, L. Hutchings, A. Singh, D.W. Vasco, M. Walters, The Northwest Geysers EGS Demonstration Project, California - Part 2: modeling and interpretation, Geothermics 63 (2016) 120–138, https://doi.org/10.1016/j.geothermics.2015.08.002.
[17] J. Rutqvist, D. Vasco, L. Myer, Coupled reservoir-geomechanical analysis of CO_2 injection and ground deformations at In Salah, Algeria, Int. J. Greenh. Gas Control 4 (2010) 225–230.
[18] J.-W. Park, J. Rutqvist, D. Ryu, E.-S. Park, J.-H. Synn, Coupled thermal-hydrological-mechanical behavior of rock mass surrounding a high-temperature thermal energy storage cavern at shallow depth, Int. J. Rock Mech. Min. Sci. 83 (2016) 149–161, https://doi.org/10.1016/j.ijrmms.2016.01.007.
[19] A. Armandine Les Landes, J. Rohmer, A. Loschetter, C. Maragna, L. Perozzi, L. Guglielmetti, T.G. Vangkilde-Pedersen, Uncertainty Management in Underground Thermal Energy Storage Development and Operation, GEOTHERMICA – ERA NET Cofund Geothermal, 2021, 73 p.
[20] HEATSTORE—final report on tools and workflows for simulating subsurface dynamics of different types of high temperature underground thermal energy storage, in: T. Driesner (Ed.), GEOTHERMICA—ERA NET Cofund Geothermal, 2021, 355 pp.
[21] P. Meier, C. Wanner, N. Dutler, F. Serbeto, N. Geissler, A. El-Alfy, A. Alcolea, L. Diamond, F. Garsche, J. Schlüsener, T. König, A. Guzik, U. Spring, D. Da Silva, C. Wilke, A. Sager, Development of the HT-ATES Heat Storage Reservoir at Bern Forsthaus, Switzerland, European Geothermal Congress, Zürich, Switzerland, 2025, 8–10 October, 2025.
[22] Model validation for subsurface dynamics, in: F. Diaz-Maurin, M.W. Saaltink (Eds.), GEOTHERMICA – ERA NET Cofund Geothermal, 2021, 110 pp.
[23] L. Manatschal, Numerical Modeling of Heat Storage in the Lower Freshwater Molasse, Thesis, ETH, Zurich, 2017.
[24] A.P. Rinaldi, J. Rutqvist, K. Luu, L. Blanco-Martín, M. Hu, M.L. Sentís, L. Eberle, P. Kaestli, TOUGH3-FLAC3D: a modeling approach for parallel computing of fluid flow and geomechanics, Comput. Geosci. 26 (2022) 1563–1580, https://doi.org/10.1007/s10596-022-10176-0.
[25] J. Rutqvist, Y.-S. Wu, C.-F. Tsang, G.A. Bodvarsson, Modeling approach for analysis of coupled multiphase fluid flow, heat transfer, and deformation in fractured porous rock, Int. J. Rock Mech. Min. Sci. 39 (2002) 429–442, https://doi.org/10.1016/S1365-1609(02)00022-9.
[26] Y. Jung, G.S.H. Pau, S. Finsterle, R.M. Pollyea, TOUGH3: a new efficient version of the TOUGH suite of multiphase flow and transport simulators, Comput. Geosci. 108 (2022) 2–7, https://doi.org/10.1016/j.cageo.2016.09.009.
[27] Itasca, Flac3d Version 6.0 - Fast Lagrangian Analysis of Continua in 3 Dimensions, ITASCA Consulting Group Inc, 2018. https://www.itascacg.com/software/flac3d.
[28] J. Rutqvist, C.-F. Tsang, Multiphysics processes in partially saturated fractured rock: experiments and models from Yucca Mountain, Rev. Geophys. 50 (2012) RG3006.
[29] L. Blanco-Martín, J. Rutqvist, J.T. Birkholzer, Extension of TOUGH-FLAC to the finite strain framework, Comput. Geosci. 108 (2017) 64–71, https://doi.org/10.1016/j.cageo.2016.10.015.
[30] H. Xu, J. Rutqvist, C. Plúa, G. Armand, J. Birkholzer, Modeling of thermal pressurization in tight claystone using sequential THM coupling: benchmarking and validation against in-situ heating experiments in COx claystone, Tunn. Undergr. Space Technol. 103 (2020) 103428, https://doi.org/10.1016/j.tust.2020.103428.
[31] B. Garitte, T.S. Nguyen, J.D. Barnichon, B.J. Graupner, C. Lee, K. Maekawa, C. Manepally, G. Ofoegbu, B. Dasgupta, R. Fedors, P.Z. Pan, X.T. Feng, J. Rutqvist, F. Chen, J. Birkholzer, Q. Wang, O. Kolditz, H. Shao, Modelling the Mont Terri HE-D experiment for the thermal–hydraulic–mechanical response of a bedded argillaceous formation to heating, Environ. Earth Sci. 76 (2017) 345, https://doi.org/10.1007/s12665-017-6662-1.
[32] B.J. Graupner, K. Thatcher, L. Friedenberg, R. Guo, T. Hadgu, W. Hou, W. Kaiser, T. Kim, C.H. Park, C. Lee, E. Matteo, T. Nagel, R. Newson, P.-Z. Pan, M. Pitz, J. Rutqvist, J. Thiedau, L. Urpi, An international study on THM modelling of the full-scale heater experiment at Mont Terri laboratory, Geomech. Energy Environ. 41 (2025) 100631, https://doi.org/10.1016/j.gete.2024.100631.
[33] C. Plúa, M.-N. Vu, G. Armand, Z. Ouraga, Z. Yu, J.-F. Shao, Q. Wang, H. Shao, T. Sasaki, S. Yoon, J. Rutqvist, F. Song, S. Collico, A. Gens, L. Bruffell, K. Thatcher, A.E. Bond, Numerical investigation of the thermal-hydrofracturing behavior of the Callovo-Oxfordian claystone, Geomech. Energy Environ. 40 (2024) 100596, https://doi.org/10.1016/j.gete.2024.100596.
[34] J. Rutqvist, B. Graupner, Y. Guglielmi, T. Kim, J. Maßmann, T.S. Nguyen, J. W. Park, W. Shiu, L. Urpi, J.-S. Yoon, G. Ziefle, J. Birkholzer, An international model comparison study of controlled fault activation experiments in argillaceous claystone at the Mont Terri Laboratory, Int. J. Rock Mech. Min. Sci. 136 (2020) 104505, https://doi.org/10.1016/j.ijrmms.2020.104505.
[35] T. Sasaki, S. Yoon, J. Rutqvist, Modelling of failure and fracture development of the Callovo-Oxfordian claystone during an in-situ heating experiment associated with geological disposal of high-level radioactive waste, Geomech. Energy Environ. 38 (2024) 100546, https://doi.org/10.1016/j.gete.2024.100546.
[36] A.P. Rinaldi, J. Rutqvist, Modeling of deep fracture zone opening and transient ground surface uplift at KB-502 CO2 injection well, In Salah, Algeria, Int. J. Greenh. Gas Control 12 (2013) 155–167 (2013).
[37] C. Chang, M.D. Zoback, A. Khaksar, Empirical relations between rock strength and physical properties in sedimentary rocks, J. Pet. Sci. Eng. 51 (2006) 223–237.
[38] A.G. Corkum, C.D. Martin, The mechanical behaviour of weak mudstone (Opalinus clay) at low stresses, Int. J. Rock Mech. Min. Sci. 44 (2007) 196–209.
[39] D. Ginosar, T. Atkinson, B. Adhikari, J. Toman, J. Podgorney, Reservoir Thermal Energy Storage Benchmarking, INL/RPT-22-69373. Rev. 3, 2023.
[40] Y. Jung, G. Shu, H. Pau, S. Finsterle, C. Doughty, TOUGH3 User's Guide Version 1.0, Energy Geosciences Division, Lawrence Berkeley National Laboratory, LBNL-2001093, 2018.
[41] M. Collignon, Ø. Strengehagen Klemetsdal, O. Møyner, M. Alcanié, A.P. Rinaldi, H. Nilsen, M. Lupi, Evaluating thermal losses and storage capacity in high-temperature aquifer thermal energy storage (HT-ATES) systems with well operating limits: insights from a study-case in the Greater Geneva Basin, Switzerland, Geothermics 85 (2020) 101773.
[42] R. Vidal, M. Saaltink, A novel method for decoupling thermo-hydraulic processes from chemical reactions to understand the effect of heat on chemical reactions, Geothermics 126 (2025) 103203.